AIP | Applied Physics Letters

Influence of the chemical surface structure on the nanoscale friction in plasma nitrided and post-oxidized ferrous alloy

Márcia Freislebem, Caren M. Menezes, Felipe Cemin, Fernanda B. Costi, Patrícia A. Ferreira, César Aguzzoli, Israel J. R. Baumvol, Fernando Alvarez, and Carlos A. Figueroa

Citation: Applied Physics Letters **105**, 111603 (2014); doi: 10.1063/1.4894803
View online: http://dx.doi.org/10.1063/1.4894803
View Table of Contents: http://scitation.aip.org/content/aip/journal/apl/105/11?ver=pdfcov
Published by the AIP Publishing

Influence of the chemical surface structure on the nanoscale friction in plasma nitrided and post-oxidized ferrous alloy

Márcia Freislebem,[1] Caren M. Menezes,[1] Felipe Cemin,[1] Fernanda B. Costi,[1] Patrícia A. Ferreira,[1] César Aguzzoli,[1] Israel J. R. Baumvol,[1,2] Fernando Alvarez,[3] and Carlos A. Figueroa[1,4,a)]

[1]*Centro de Ciências Exatas e Tecnologia, Universidade de Caxias do Sul, Caxias do Sul-RS 95070-560, Brazil*
[2]*Instituto de Física, Universidade Federal do Rio Grande do Sul, Porto Alegre-RS 91509-970, Brazil*
[3]*Instituto de Física "Gleb Wataghin," Universidade Estadual de Campinas, Campinas-SP 13081-970, Brazil*
[4]*Plasmar Tecnologia Ltda., Caxias do Sul-RS 95076-420, Brazil*

(Received 16 March 2014; accepted 16 August 2014; published online 16 September 2014)

Friction is a ubiquitous phenomenon in everyday activities spanning from vehicles where efficient brakes are mandatory up to mechanical devices where its minimum effects are pursued for energy efficiency issues. Recently, theoretical models succeed correlating the friction behavior with energy transference via phonons between sliding surfaces. Therefore, considering that the energy losses by friction are prompted through phonons, the chemical surface structure between sliding surfaces is very important to determine the friction phenomenon. In this work, we address the issue of friction between a conical diamond tip sliding on different functionalized flat steel surfaces by focusing the influence of the chemical bonds in the outermost layers on the sliding resistance. This geometry allows probing the coupling of the sharp tip with terminator species on the top and underneath material surface at in-depth friction measurements from 20 to 200 nm. Experimentally, the friction coefficient decreases when *nitrogen* atoms are *substituted* for *oxygen* in the iron network. This effect is interpreted as due to energy losses through phonons whilst lower vibrational frequency excitation modes imply lower friction coefficients and a more accurate adjustment is obtained when a theoretical model with longitudinal adsorbate vibration is used. © *2014 AIP Publishing LLC*. [http://dx.doi.org/10.1063/1.4894803]

Nowadays, the energy efficiency is a crucial issue to save natural and economical resources, improving the lifetime of material systems, and developing intelligent materials and surfaces.[1–3] Energy efficiency is mainly relevant for mechanical systems where solid surfaces are in contact and the friction control is mandatory in order to diminish energy losses.

There are three different scales in tribology, namely, macroscopic, microscopic, and nanoscopic, each of them leading to different conceptions of the friction phenomenon. The macroscopic properties influencing friction such as hardness, elastic modulus, and shear stress are not obviously correlated with fundamental properties of materials. For instance, bond strength, phonons and electrical (thermal) conductivity properties are not in general considered in friction studies from an engineering point of view. In fact, incorporation of fundamental physical concepts at the nanoscale friction studies started two decades ago.[4–7] Recently, by applying a chemical approach, a *qualitative* correlation between the friction coefficient of several oxides with the ionic surface potential relationship was established.[8,9] Also, the influence of phonons has been incorporated in the effort to understand the friction phenomenon at the nanoscale level, i.e., by considering the excitation of vibrational modes of the atoms bonded at the studied surfaces.[6] These authors succeed correlating the vibrational frequency modes of terminator species at the surface and the friction phenomenon. According to this model, the mechanical energy transference between sliding surfaces is dissipated via phonons. Understanding friction in terms of elementary vibrational frequency modes of chemical bonds may open pathways to tailoring sliding material surfaces. Indeed, specifically functionalized surfaces by chemical treatment will help decreasing the phonon coupling strength and thus decreasing the friction coefficient.

In this work, we address the issue of friction between a conical diamond tip sliding on different functionalized flat steel surfaces by focusing the influence of the chemical bonds (i.e., elementary vibrational frequency modes coupling) on the sliding resistance. This particular geometry allows probing the coupling of the sharp tip with the terminator species on the top and underneath of the material at nanoscale level from 20 to 200 nm. The in-depth friction dependence on material composition and microstructure was studied in plasma nitrided and post-oxidized steel samples and correlated with the material chemical bonding of the modified cases.

The samples were cut from 12 mm diameter AISI 1045 plain steel bar (C, 0.49; Si, 0.26; P, 0.002; S, 0.009; Mn, 0.68; Cu, 0.07; Cr, 0.01; Ni, 0.03; Mo, 0.005; Al, 0.002; V, 0.005; balance Fe (wt. %)). The substrates were mirror polished (colloidal silica) by standard metallographic techniques. Nitriding was performed in a laboratory scale chamber (base pressure ≤ 2 Pa). The chamber feeding gases are controlled by mass flow controllers keeping a total pressure of 100 Pa and using a gaseous mixture 90% N_2 and 10% H_2 during nitriding process. The working temperature during the nitriding process was kept at 550 ± 5 °C for 5 h. A DC

a)E-mail: cafiguer@ucs.br. Phone: ++55-54-91796-022.

power supply with mean voltage of 500 V and current density of 1.2 mA cm^{-2} was used. Following nitriding, post-oxidation was performed in the same chamber, without opening it. Two types of samples were produced. One was just nitrided and the other nitrided and post-oxidizing during 1 min at a constant temperature of 480 ± 4 °C. The total gas pressure was kept at 174 Pa and the gas mixture was 65% N_2, 25% H_2, and 10% O_2 during post-oxidizing process. A DC power supply with mean voltage of 800 V and current density of 2.0 mA cm^{-2} was used.

The composition chemical profiles of the modified samples were obtained by glow discharge optical emission spectroscopy (GD-OES, Horiba, GD Profiler 2) by measuring the emission intensities of chemical elements present in the sample surface. The measurements were performed at 630 Pa and 30 W with an acquisition time of 120 s. The crystalline structures of the plasma-modified outermost layers were characterized by X-ray diffraction (XRD) at grazing angle incidence ($\theta = 2°$). The samples were rotated during analysis in order to reduce grain orientation and texture effects. A Shimadzu XRD-6000 diffractometer with Cu Kα (V = 40 kV and I = 30 mA) radiation was used. The morphology and microstructure of nitrided and oxidized layers were accessed by scanning electron microscopy (SEM) in secondary electron mode (Shimadzu SSX-550). For SEM analysis, the cross-section of samples was revealed by attacking the surface at room temperature with Nital solution (5%). The modified layers thicknesses were determined from the SEM images. The hardness was measured by a NanoTest-600 equipment (MicroMaterials, Berkovich diamond indenter) in an average indentation depth of 100 nm and the indentation curves were analyzed by the Oliver and Pharr method.[10] An initial load of 0.03 mN and a loading rate of 0.05 mN s^{-1} were applied. The surface roughness and friction measurements were obtained in sliding tests, using the same apparatus by adding a load cell (probe) and replacing the Berkovich diamond indenter by a conical diamond tip with a final radius of 25 μm. In these experiments, normal loads of 10, 15, and 20 mN were applied and the samples were displaced at a rate of 1 μm s^{-1} to a total distance of 680 μm. The tangential force was measured and its average steady-state value was correlated to the friction force applied by the layer formed on the functionalized sample surfaces. The results presented in the letter are the average from ten measurements performed for each applied normal load and using two different friction probes (load cell). The indentation depths vary from 20 to 200 nm. The temperature and humidity for all hardness and friction measurements were 23 °C and 50% ± 5%, respectively.

Figure 1 shows the X-ray diffraction patterns at grazing angle (2°) obtained from the only nitrided and nitrided and post-oxidized samples. Considering the grazing angle and the material type, the value information is roughly coming from 800 nm depth. The diffraction patterns are formed by a mixture of phases such as iron nitrides γ'-Fe_4N and ε-$Fe_{2\text{-}3}N$ in both samples. Also, only one type of iron oxide, i.e., magnetite (Fe_3O_4) is formed in the plasma post-oxidized sample.

Figure 2 shows the cross-section scanning electron microscopy images showing the near-surface structure of the

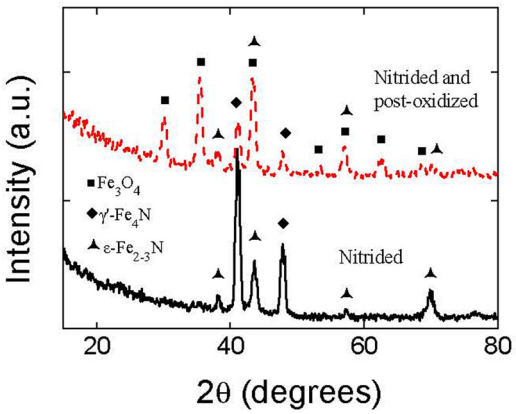

FIG. 1. X-ray diffraction patterns at grazing angle ($\Theta = 2°$) for the nitrided and the nitrided and post-oxidized samples.

treated samples, i.e., (a) the only nitrided and (b) the nitrided and post-oxidized samples. For completeness, the relative chemical profiles for nitrogen and oxygen in both samples obtained by GD-OES is superimposed on the images. According to both techniques, the outermost layer of the only nitrided and post-oxidized samples contains nitrogen and oxygen, respectively. The oxide layer constituted only by magnetite, has an average thickness of ~230 nm. The oxygen signal recorded in the only nitrided sample is due to atmospheric oxygen physisorption (Figure 2(a)).

Table I shows the hardness, elastic modulus, plasticity index, and surface roughness of both samples at an average depth of 120 nm. These macroscopic mechanical properties, within the experimental errors, are constant in the range where the friction measurements were performed. In spite of the main macroscopic properties controlling the friction are constant, the friction coefficients measured in both types of samples are different. These findings suggest that we have to investigate at a lower level scale to understand the physical causes of the friction differences obtained from the nanoindentation experiments, i.e., the friction differences are related directly to the atomic species involved in the friction phenomenon. It is important to stress that the lubricious property of oxide layer coating metals is well known in tribology applications.[11] This suggests that outermost oxidized layer is not only a simple barrier but also intervening on the physical and/or chemical properties that must be taken into account in sliding surfaces. Moreover, the friction force at the nanoscale depends linearly on the number of atoms that

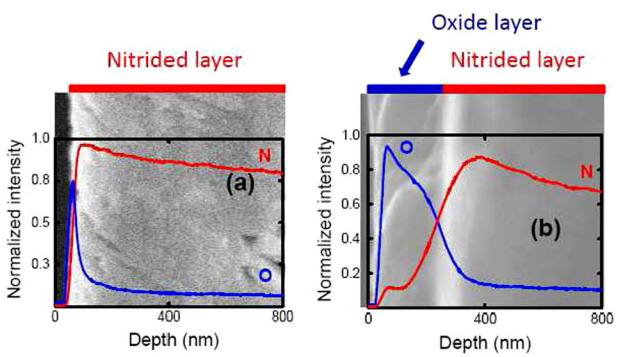

FIG. 2. SEM cross section images for (a) the nitrided and (b) the nitrided and post-oxidized sample. The relative O and N profiles obtained by GD-OES are superposed.

TABLE I. Hardness, elastic modulus (E), plasticity index, and surface roughness (Rq) measured for both samples at an average depth of 120 nm.

Sample	Nitrided	Nitrided and post-oxidized
Hardness (GPa)	9.4 ± 2.5	9.3 ± 1.5
E (MPa)	240 ± 10	252 ± 26
Plasticity index	6.4 ± 0.7	6.3 ± 0.7
Rq (nm)	175 ± 14	171 ± 16

chemically interact across the contact.[12] Therefore, the chemical specificity of the terminator should be invoked in order to obtain quantitative information of the friction issue. In our case, the observed friction differences in the studied samples are attributed to the presence of oxygen instead of nitrogen in the iron network. As remarked above and from a tribological point, strength, toughness fracture, hardness, and elastic modulus are macroscopic properties that influence the friction coefficient by essentially adhesive and ploughing phenomena.[1] From a physicochemical point of view, the macroscopic properties cited above can be understood in terms of elementary interactions such as attractive forces (Van der Waals), strength and stiffness of chemical bonds, thermal (electrical) conductivities involving phonons coupling, and electronic band structures.[7] According to recent models considering elementary vibrational frequencies modes of bonded atoms forming the outermost layer of the material, the friction force due to vibrational damping is giving by $F = m\eta v$, where $\eta = m\omega^4/2\pi\rho\ C_T^3$ is the damping constant in the case of a single adsorbate[5] and $\eta_\perp = m\omega^2 n_a/\rho\ C_L$ in the case of ordered commensurate adsorbate layers with longitudinal elastic waves.[13,14] Here, m is the mass of adsorbate, ω is the vibrational frequency, ρ is the density, n_a is the number of adsorbates per unit area, C_T and C_L are the material transverse and longitudinal sound velocity, respectively, and v is the relative sliding surface velocity. Therefore, although that there is not enough experimental information to draw the absolute friction force, the ratio $F_{N\text{-}Fe}/F_{O\text{-}Fe}$ can give us insight about the relative influence of the terminator species on the process. In order to do this, we shall assume the following. First, the sound velocities C_T and C_L are 3232 and 6081 m s^{-1} (for nitrides[15,16]) and 3555 and 7110 m s^{-1} (for magnetite[17] and considering $C_T \cong C_L/2$ for the C_T[14]), respectively. Second, the nitrides are assumed to be formed by a 50% of the constituting nitride phases (γ-$Fe_4N + \varepsilon$-$Fe_{2\text{-}3}N$) and both surfaces have the same n_a. Third, the nitrides and magnetite densities are 6.35 and 5.15 g cm^{-3}, respectively,[18,19] and the two masses of adsorbates are 14 and 16 g mol^{-1} for nitrogen and oxygen, respectively. Finally, the more intense vibrational frequency modes 779 cm^{-1} (nitrides) and 668 cm^{-1} (magnetite) are considered

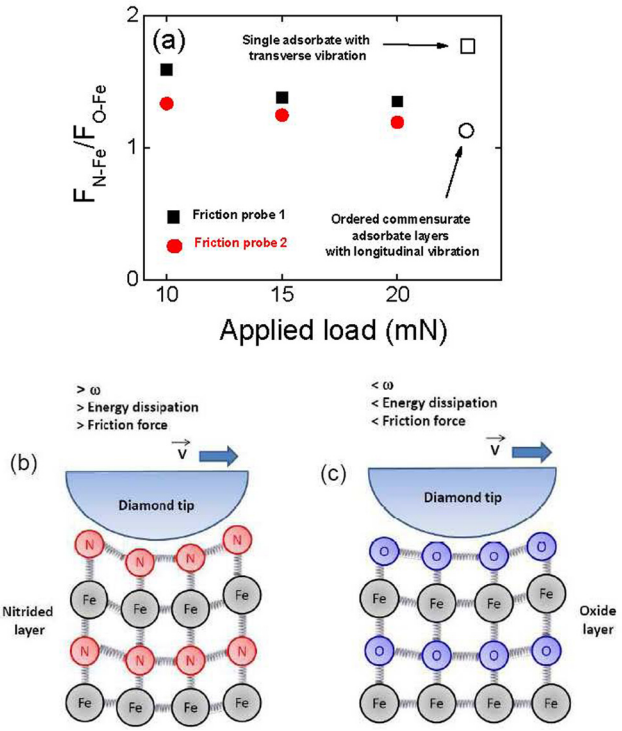

FIG. 3. (a) Ratio $F_{N\text{-}Fe}/F_{O\text{-}Fe}$ as a function of applied load. The experimental error is in the order of the size of the symbols. The empty square and circle correspond to results after the application of phonon coupling models obtained from the single adsorbate with transverse vibrations and ordered commensurate adsorbate layers for longitudinal vibrations, respectively. (b) and (c) Schematic of the sliding of a conical tip on outermost layers of ion nitride and iron oxide, respectively.

responsible for the coupling interaction between the sliding surfaces.[20,21]

Table II shows a comparison among both models and experimental results by considering the ratio $F_{N\text{-}Fe}/F_{O\text{-}Fe}$. One can see that the friction coupling is stronger on the surface containing N than the one containing O whatever the value of the ratio $F_{N\text{-}Fe}/F_{O\text{-}Fe}$ be considered either from theoretical models or experimental results.

As explained above, these data were obtained with two different friction probes in order to improve the measurement statistic and the individual ratios at different applied normal loads (please, see Figure 3(a)). For completeness, the theoretical results obtained by using the models of the single adsorbate for transverse vibrations and the ordered commensurate adsorbate layers for longitudinal vibrations are also shown. Moreover, Figures 3(b) and 3(c) show a schematic of the sliding of a conical diamond tip on outermost layers of iron nitride and iron oxide, respectively. From these results one can conclude the following. First, the theoretical model of single adsorbate provides an overestimated value of 37%,

TABLE II. Comparison of the ratio $F_{N\text{-}Fe}/F_{O\text{-}Fe}$ calculated from two different theoretical models and obtained by experimental measurements in both surfaces (N-Fe and O-Fe).

	$F_{N\text{-}Fe}/F_{O\text{-}Fe}$	Difference with the experimental value
Model I: single adsorbate (transverse vibration)	1.75	37%
Model II: ordered commensurate adsorbate layers (longitudinal vibration)	1.13	14%
Experimental measurements (average of two different friction probes)	1.29	0

whereas the model of ordered commensurate adsorbate layers provides an underestimated value of 14% when compared to the average of experimental results obtained by using two different friction probes. Second, the results are well resolved clearly showing the influence of the terminator species on the friction coefficient and the theoretical model, which provides the best approximation to the experimental results (14%), takes into account perpendicular adsorbate vibrations coupling with longitudinal elastic waves. Therefore, these results are in agreement with the experiments obtained from the perpendicular indented conical tip sliding on the surface at depths between 20 and 200 nm (i.e., probing an average of 1200 atomic layers). Finally, an important conclusion is that the perpendicular contact (i.e., prompting longitudinal vibration component) is rather more important than the sliding (i.e., prompting transverse vibration component) between surfaces in terms of the friction coupling of our system and controls the energy dissipation mechanism.

In conclusion, the nanoscale friction results are interpreted by assuming a coupling, via elementary vibrational frequency modes of the terminator atoms, between the sliding tip and the functionalized surface. Consequently, the friction coefficient for the post-oxidized sample decreases when *nitrogen* atoms are *substituted* for *oxygen*, i.e., the chemical bonds in the outermost layers prompt the friction coefficient via elementary vibration modes coupling between sliding surfaces in physical contact. A theoretical model that considers perpendicular adsorbate vibrations provides the best approximation and is in agreement with the experimental arrangement of in-depth friction measurements from 20 to 200 nm.

These remarkable findings may open pathways to chemical tailoring surface materials (*functionalization*) in order to reduce friction and energy losses as long as the macroscopic mechanical properties such as hardness, elastic modulus, plasticity index, and surface roughness remain constant.

The authors are grateful to UCS, INCT-INES (CNPq), CAPES, FAPERGS for financial support. C.M.M., F.B.C., P.A.F., F.C., I.J.R.B., F.A., and C.A.F. are CNPq and CAPES fellows. F.A. is in part supported by Fapesp Project 2012/10127-5.

[1]K. Holmberg, R. Siilasto, T. Laitinen, P. Andersson, and A. Jäsberg, Tribol. Int. **62**, 58 (2013).
[2]K. Holmberg, P. Andersson, and A. Erdemir, Tribol. Int. **47**, 221 (2012).
[3]M. Sabeur, D. Ibrahim, E. M. Mohamed, and Z. Hassan, Tribol. Int. **59**, 240 (2013).
[4]K. Holmberg and A. Matthews, *Coatings Tribology: Properties, Mechanisms, Techniques and Applications in Surface Engineering* (Elsevier, 2009).
[5]R. J. Cannara, M. J. Brukman, K. Cimatu, A. V. Sumant, S. Baldelli, and R. W. Carpick, Science **318**, 780 (2007).
[6]B. N. J. Persson, F. Bucher, and B. Chiaia, Phys. Rev. B **65**, 184106 (2002).
[7]J. Krim, Adv. Phys. **61**, 155 (2012).
[8]A. Erdemir, Surf. Coat. Technol. **200**, 1792 (2005).
[9]A. Erdemir, S. Li, and Y. Jin, Int. J. Mol. Sci. **6**, 203 (2005).
[10]W. C. Oliver and G. M. Pharr, J. Mater. Res. **7**, 1564 (1992).
[11]P. J. Blau, *Friction Science and Technology: From Concepts to Applications* (CRC Press, 2009).
[12]Y. Mo, K. T. Turner, and I. Szlufarska, Nature **457**, 1116 (2009).
[13]S. P. Lewis, M. V. Pykhtin, E. J. Mele, and A. M. Rappe, J. Chem. Phys. **108**, 1157 (1998).
[14]B. N. J. Persson, E. Tosatti, D. Fuhrmann, G. Witte, and Ch. Wöll, Phys. Rev. B **59**, 11777 (1999).
[15]Y.-J. Shi, Y.-L. Du, and G. Chen, Comput. Mater. Sci. **67**, 341 (2013).
[16]R. Niewa, D. Rau, A. Wosylus, K. Meier, M. Hanfland, M. Wessel, R. Dronskowski, D. A. Dzivenko, R. Riedel, and U. Schwarz, Chem. Mater. **21**, 392 (2009).
[17]S. Isida, M. Suzuki, S. Todo, N. Môri, and K. Siratori, Physica B **219–220**, 638 (1996).
[18]E. A. Ochoa, D. Wisnivesky, T. Minea, M. Ganciu, C. Tauziede, P. Chapon, and F. Alvarez, Surf. Coat. Technol. **203**, 1457 (2009).
[19]W. L. Roberts, *Encyclopedia of Minerals* (Chapman & Hall, 1990).
[20]G. V. Chertihin, L. Andrews, and M. Neurock, J. Phys. Chem. **100**, 14609 (1996).
[21]O. N. Shebanova and P. J. Lazor, Solid State Chem. **174**, 424 (2003).